# Beam energy dependence of the squeeze-out effect on the directed and elliptic flow in Au + Au collisions in the high baryon density region

Chao Zhang (张潮),[1] Jiamin Chen (陈佳敏),[1] Xiaofeng Luo (罗晓峰),[1,*] Feng Liu (刘峰),[1] and Yasushi Nara (奈良寧)[2,3]
[1]*Institute of Particle Physics and Key Laboratory of Quark & Lepton Physics (MOE), Central China Normal University, Wuhan 430079, China*
[2]*Akita International University, Yuwa, Akita-city 010-1292, Japan*
[3]*Frankfurt Institute for Advanced Studies, D-60438 Frankfurt am Main, Germany*

(Received 11 March 2018; revised manuscript received 23 April 2018; published 18 June 2018)

We present a detailed analysis of the beam energy dependence of the mechanisms for the generation of directed and elliptic flows in Au + Au collisions focusing on the role of hadronic rescattering and spectator shadowing within a microscopic transport model JAM with different equations of state. A systematic study of the beam energy dependence is performed for Au + Au collisions at $\sqrt{s_{NN}} = 2.3 - 62.4$ GeV. The transition of the dynamical origin of the directed flow is observed. We find that the initial Glauber-type nucleon-nucleon collisions generate negative $v_1$ for nucleons at midrapidity due to the presence of spectator matter, and this negative nucleon $v_1$ is turned to be positive by the meson-baryon interactions at the beam energy region of $\sqrt{s_{NN}} < 30$ GeV. In contrast, above 30 GeV there is no spectator shadowing at midrapidity, and initial nucleon-nucleon collisions do not generate directed flow, but subsequent rescatterings among produced particles generate negative $v_1$ for nucleons. It is demonstrated that negative pion-directed flows are mostly generated by the interaction with the spectator matter. It is also shown that the squeeze-out effect is largely suppressed in the case of softening, which leads to the enhancement of elliptic flow around $\sqrt{s_{NN}} = 5 - 7$ GeV. The elliptic flow at midrapidity above 10 GeV is not influenced by the squeeze-out due to spectator matter, while its effect is seen at the forward rapidity range of $y/y_{\text{c.m.}} > 0.5$, which decreases as beam energy increases.

DOI: 10.1103/PhysRevC.97.064913

## I. INTRODUCTION

A new form of strongly interacting dense QCD matter called quark-gluon plasma (QGP) is created in the experiments in high-energy heavy ion collisions at the Relativistic Heavy Ion Collider (RHIC) and Large Hadron Collider (LHC) [1–3]. The lattice QCD calculations confirmed that at zero baryon density, the transition from hadronic matter to QGP is a crossover [4]. The next challenge is to explore the phase diagram of QCD matter extending to finite baryon density regions by creating compressed baryonic matter (CBM) [5]. At nonvanishing baryon densities, a first-order and/or second-order QCD phase transition together with a critical end point have been speculated by many theoretical calculations [6]. A first-order phase transition implies the existence of a strong softest point in the equation of state (EoS) [7,8], and it is conjectured that this softening effects may be seen in observables. To find the evidence of a phase transition and the presence of a critical end point, various observables have been measured such as particle ratios, moments of the conserved charges, and collective flows [9–11]. New CBM experiments are planned such as Beam Energy Scan (BES II) at RHIC [12], Facility for Antiproton and Ion Research (FAIR) [13,14], Japan Proton Accelerator Research Complex for Heavy Ion (J-PARC-HI) [15], SPS Heavy Ion and Neutrino Experiment (NA61-SHINE) at the Super-Proton Synchrotron (SPS) [16], and Nuclotron-based Ion Collider fAciilty (NICA) [17] to explore the phase diagram at high baryon density region.

In this paper, we focus on anisotropic collective flows. An analysis of the anisotropic collective flows [18,19] in noncentral nuclear collisions appears to be one of the most popular methods in studying the properties of the hot and dense matter since they are sensitive to the EoS in the early stages of nuclear collisions [20,21], and thus considered to be a good probe to explore the properties of the QCD matters. The anisotropic flows are defined by the Fourier coefficients of the expansion of the azimuthal distribution of particles measured with respect to the reaction plane, which is spanned by the vector of the impact parameter and the beam direction [22–24]

$$E\frac{d^3N}{d^3p} = \frac{1}{2\pi}\frac{d^2N}{p_T dp_T dy}\left[1 + 2\sum_{n=1}^{\infty} v_n \cos n[(\phi - \Psi_{\text{RP}})]\right], \tag{1}$$

where $\phi$ is the azimuthal angle, and $\Psi_{\text{RP}}$ is the reaction plane azimuthal angle. The flow coefficients $v_n = \langle \cos n[(\phi - \Psi_{\text{RP}})]\rangle$ characterize the event anisotropy. The directed flow parameter is defined as the first Fourier coefficient $v_1$ of the particle momentum distribution, and the second coefficient $v_2$ is referred to as elliptic flow.

Directed flow is very sensitive to the early dynamics of the heavy ion collisions [24]. The excitation function of the nucleon directed flow at midrapidity is predicted to have a minimum at a certain collision energy in the hydrodynamical calculations with a first-order phase transition (1OPT)

*xfluo@mail.ccnu.edu.cn

 

[8,25,26]. Furthermore, when the system passes through the softest point of the EoS, the slope of the directed flow for nucleons turns to be negative [25,27,28], which is called the third flow [28,29] or the antiflow of nucleon [25,27]. This does not happen for the crossover transition [30]. Hence, it is predicted that the collapse of the directed flow is a signature of a QCD first-order phase transition. The negative slope of protons in a first-order phase transition has been also confirmed within a microscopic transport model JAM, in which the effects of EoS is incorporated by changing a scattering style in the two-body collisions [31,32]. Recent measurements by the STAR Collaboration [33,34] show negative proton $v_1$ at above $\sqrt{s_{NN}} \approx 10$ GeV in the energy range of RHIC-BES program. We note that in the microscopic transport models RQMD [35], UrQMD [36], and PHSD/HSD [37], the negative slope of proton $v_1$ at midrapidity is found at high bombarding energies $\sqrt{s_{NN}} \geqslant 27$ GeV, which is caused by the certain amount of degree of rapidity loss of incoming nucleons and positive space momentum correlation [35]. At the bombarding energies of $\sqrt{s_{NN}} \leqslant 20$ GeV [37,38], such microscopic transport models do not show a negative slope for nucleons. Therefore, the negative proton $v_1$ slope at midrapidity at $\sqrt{s_{NN}} \leqslant 20$ GeV can be only produced by theoretical models which incorporate the effect of a first-order phase transition.

The elliptic flow also provides information about the early stages of the collision [39–42], and it is one of the most extensively studied observables in relativistic nucleus-nucleus collisions. At lower beam energies of $E_{\rm lab} \leqslant 5$ AGeV, shadowing effects by the spectator matter have been known to play an essential role for directed and elliptic flows. It is known that the reflection of pion by the nucleon is the dominant origin of the negative directed flow for pions [43] at $E_{\rm lab} \approx 1-2$ AGeV. The presence of spectator matter is the origin of the squeeze-out (out-of-plane emission) [44,45], and elliptic flow can be even negative at lower energies. In the high baryon density region, such as the Alternating Gradient Synchrotron (AGS) energies, the final strength of the elliptic flow is determined by the interplay between the squeeze-out effect and in-plane emission [39]. Enhancement of elliptic flow due to the softening of EoS is predicted [46,47], because softening of EoS suppresses the squeeze-out effect.

So far a systematic study of the role of spectator matter for a wide range of beam energies has not been performed. In this paper, we shall study in detail the role of spectator shadowing on both the directed and elliptic flows, together with its EoS dependence. For this purpose, we utilize a microscopic transport model JAM to systematically study the collision dynamics emphasis on the effects of EoS, hadron rescattering, hadronic mean-field, and interaction with spectator to the anisotropic collective flows in Au + Au collision at $\sqrt{s_{NN}} = 2.3-62.4$ GeV. We shall show that the shadowing effect by the spectator still plays an important role for the generation of anisotropic flows at RHIC-BES energies of $\sqrt{s_{NN}} < 30$ GeV. We investigate such effects by disabling meson-baryon ($MB$), and meson-meson ($MM$) collisions, as well as the interactions between participants and spectator matter.

The paper is organized as follow. After the brief description of the JAM model in Sec. II, we compute the rapidity and transverse momentum distributions of identified particles with different EoS in Sec. III. In Sec. IV, hadronic rescattering and spectator effects together with EoS dependence are discussed for Au + Au collisions at $\sqrt{s_{NN}} = 5$ GeV. Then we investigate the beam energy dependence of the spectator shadowing on the directed and elliptic flows in Sec. V. Finally, a summary will be given in Sec. VI.

## II. JAM MODEL

We employ a hadronic transport model JAM [48] that is developed to simulate relativistic nuclear collisions from initial stage to final state interaction in the hadronic gas stage. Similar to other transport models [49–53], the particle production in JAM is modeled by resonance and string production and their decay, and the particles including produced ones can interact with each other by the two-body collisions [54].

The effects of the equation of state have been implemented by two different approaches: the nuclear mean-field and modified two-body scatterings. The nuclear mean-field potential is implemented along the lines of the simplified version [55,56] of the relativistic quantum molecular dynamics approach [57]. In this approach, our Hamiltonian is given by the sum of the single-particle energy

$$H = \sum_{i=1}^{N} \sqrt{\boldsymbol{p}_i^2 + m_i^2 + 2m_i V_i} \tag{2}$$

and the following equations of motion

$$\frac{d\boldsymbol{r}_i}{dt} = \frac{\partial H}{\partial \boldsymbol{p}_i} = \frac{\boldsymbol{p}_i}{p_i^0} + \sum_{j=1}^{N} \frac{m_j}{p_j^0} \frac{\partial V_j}{\partial \boldsymbol{p}_j},$$
$$\frac{d\boldsymbol{p}_i}{dt} = -\frac{\partial H}{\partial \boldsymbol{r}_i} = -\sum_{j=1}^{N} \frac{m_j}{p_j^0} \frac{\partial V_j}{\partial \boldsymbol{r}_j}. \tag{3}$$

are numerically solved. The relative distances in the two-body center-of-mass frame are used in the argument of the potentials $V_i$:

$$-q_{Tij}^2 = -(q_i - q_j)^2 + \frac{[(q_i - q_j)\cdot(p_i + p_j)]^2}{(p_i + p_j)^2}, \tag{4}$$

$$-p_{Tij}^2 = -(p_i - p_j)^2 + \frac{[(p_i - p_j)\cdot(p_i + p_j)]^2}{(p_i + p_j)^2}, \tag{5}$$

where $q_i$ and $p_i$ are the four-vectors for the coordinate and momentum of the $i$-th particle, respectively. For the potential $V_i$, the Skyrme-type density-dependent and Lorentzian-type momentum-dependent mean-field potential [58] are implemented in the model [59,60]. In this work, we use the parameter set used in Ref. [60], which yields the nuclear incompressibility of $K = 272$ MeV.

As a second approach, we control the pressure of the system by changing the scattering style in the two-body collisions [42]. The pressure of the system with volume $V$ in which only two-body scatterings happen can be estimated by the Virial theorem [61]

$$P = P_f + \frac{1}{3TV} \sum_{(i,j)} (\boldsymbol{p}_i' - \boldsymbol{p}_i)\cdot(\boldsymbol{r}_i - \boldsymbol{r}_j) \tag{6}$$

during the time interval $T$, where $(\boldsymbol{p}_i' - \boldsymbol{p}_i)$ is a momentum transfer, and $(\boldsymbol{r}_i - \boldsymbol{r}_j)$ is a relative coordinate between two colliding particles $i$ and $j$ in the center-of-mass frame. $P_f$ is the pressure from the free streaming contribution. Thus the repulsive orbit $(\boldsymbol{p}_i' - \boldsymbol{p}_i)\cdot(\boldsymbol{r}_i - \boldsymbol{r}_j) > 0$ enhances the pressure, while the attractive orbit $(\boldsymbol{p}_i' - \boldsymbol{p}_i)\cdot(\boldsymbol{r}_i - \boldsymbol{r}_j) < 0$ reduces the pressure. In the standard transport approach, the azimuthal angle of the two-body scattering is randomly chosen. Consequently, the pressure generated by this scattering is zero in average which leads to the free hadron gas EoS. This immediately implies that one can control the pressure by appropriately choosing the scattering style. The selection of the repulsive orbit in the two-body collision [62–64] can simulate the effect of repulsive potentials. While it is shown that selecting attractive orbit for all two-body scattering yields the compatible amount of softening of a EoS with a first-order phase transition, thus it mimics the effects of a first-order phase transition [31]. In this work, the "attractive orbit" mode in JAM refers to the simulation in which attractive orbits are selected for all two-body scatterings without imposing any conditions.

The EoS of the system can be controlled by the formula in Ref. [42] by the following constraints in the two-body scattering:

$$\Delta P = \frac{\rho}{3(\delta\tau_i + \delta\tau_j)}(\boldsymbol{p}_i' - \boldsymbol{p}_i)\cdot(\boldsymbol{r}_i - \boldsymbol{r}_j)\,, \tag{7}$$

where $\Delta P$ is the pressure difference from the free streaming pressure, $\rho$ is the local particle density, and $\delta\tau_i$ is the proper time interval of the $i$-th particle between successive collisions. We show that a given EoS can be simulated by choosing the azimuthal angle according to the constraint in Eq. (7) in the two-body scattering process [32]. The main advantage of this approach is to be able to simulate any given EoS with a numerically efficient way as far as there are many two-body collisions, which happens in heavy-ion collision such as Au + Au collisions. We use the same EoS used in Ref. [32] to simulate 1OPT (JAM/1OPT) based on Eq. (7) in this paper.

## III. EFFECTS OF HADRONIC MEAN FIELDS AND SOFTENING

In this section, we investigate the effects of EoS on the spectra of identified particles by utilizing the mean-field simulation and modified scattering style approach.

### A. EoS dependence

We first compare the transverse mass spectrum and the rapidity distribution of identified particles including protons, pions, and kaons to see the effects of EoS on the gross dynamics of the collision. Figure 1(a) shows the transverse mass distribution at midrapidity $|y| < 0.12$ for $p + \bar{p}$, $\pi^+ + \pi^-$ and $K^+ + K^-$ in midcentral (10–40%) Au + Au collision at $\sqrt{s_{NN}} = 5$ GeV from JAM cascade, mean-field potential, and attractive orbit simulations. The softening effect predicts the enhancement of the collective transverse flow for all particles. This is understood by the longer interaction time due to the slow compression and expansion of the system [47] by the softening. Radial flow is generated from early to later stages of the collisions, unlike anisotropic flows which are sensitive to the early pressure. In addition, it is also proportional to the

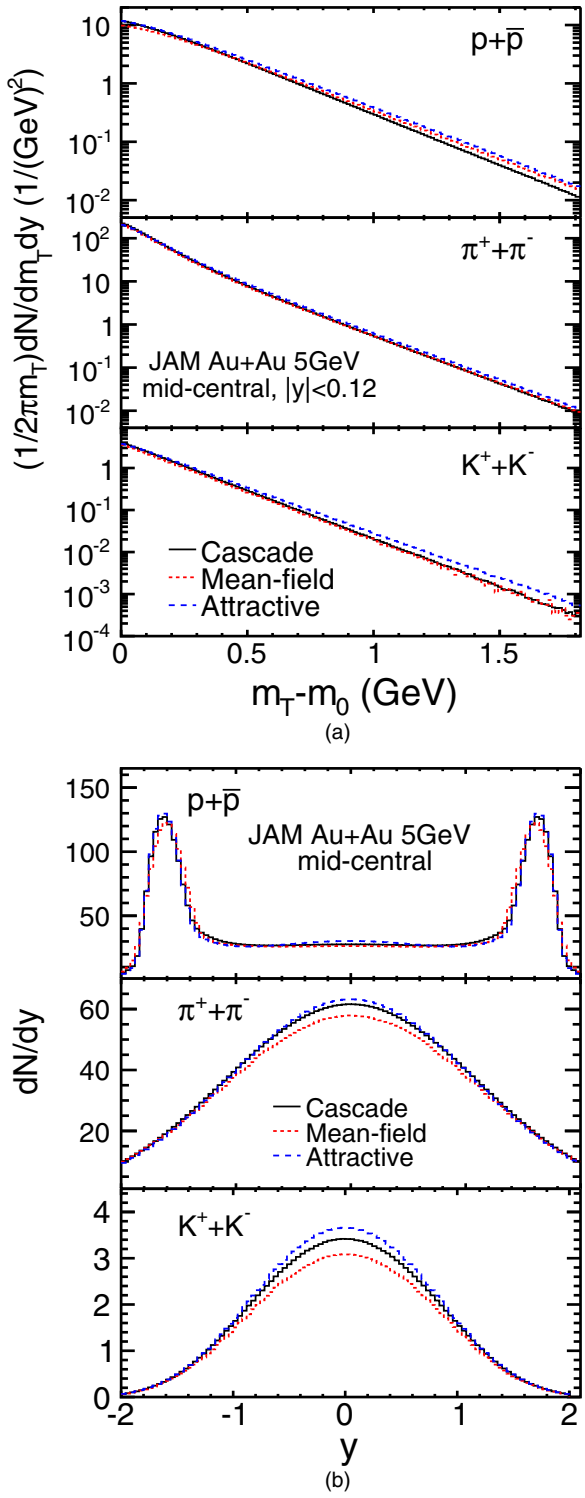


FIG. 1. (a) Transverse momentum spectrum at midrapidity ($|y| < 0.12$) and (b) rapidity distributions of identified particles; proton, pion, kaon in midcentral (10–40%) Au + Au collision at $\sqrt{s_{NN}} = 5$ GeV from JAM are compared to different EoS; cascade with mean-field potential and cascade with attractive orbit mode.

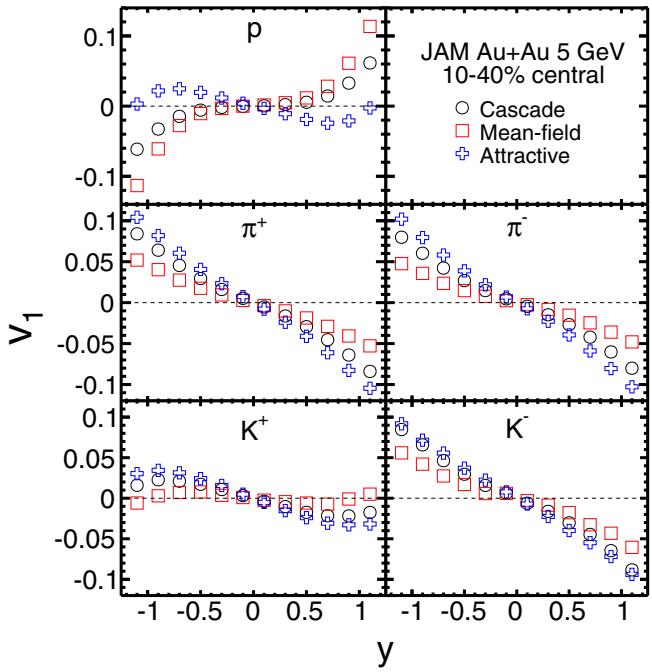


FIG. 2. Directed flows as a function of rapidity in midcentral (10–40%) Au + Au collision at $\sqrt{s_{NN}} = 5$ GeV from JAM cascade (circles), JAM with mean-field potential (squires), and JAM cascade with attractive orbit (crosses). The left and right panels show the results for identified particles $p$, $\pi^+$, $K^+$ and antiparticles $\pi^-$, $K^-$, respectively.

$pdV$ work, thus the radial flow gets larger as the system volume becomes larger. The enhancement of the transverse flow is also reported within hydrodyanmical approaches with a first-order phase transition [65–67]. JAM with hadronic mean-field mode also predicts the harder slope of protons, which is due to the repulsive potential.

Rapidity distributions of identified particles are displayed in Fig. 1(b). The softening effect is also seen in the rapidity distributions for all particles: protons, pions, and kaons yield are enhanced at midrapidity, while it is reduced at forward rapidity region making total particle yields the same. The effect of the hadronic mean-field is opposite: it reduces the particle yield at midrapidity, while it enhances the yield at the forward region.

We see some effects of EoS on the transverse momentum and rapidity distributions, but it is not a sizable effect. However, the EoS effect is dramatic for the collective flows. Sensitivities of the EoS on the elliptic flows of identified particles are studied in Ref. [46].

In Fig. 2, rapidity dependence of the directed flows for identified particles ($p$, $\pi^+$, $K^+$) and corresponding antiparticles ($\pi^-$, $K^-$) in midcentral (10–40%) Au + Au collision at $\sqrt{s_{NN}} = 5$ GeV are compared to different JAM modes: cascade, mean-field potential, and cascade with attractive orbit. It is seen that the attractive orbit simulation predicts a negative slope of protons, which is consistent with the results from a first-order phase transition in Ref. [47]. However, the mean-field potential enhances the positive $v_1$ slope for protons due to the repulsive potential, whereas, it reduces the slope for pions and kaons.

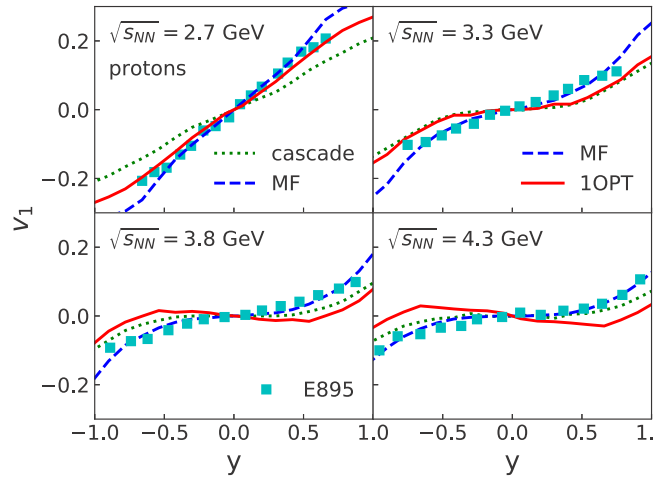


FIG. 3. Directed flows of protons as a function of rapidity in midcentral (10–40%) Au + Au collisions at $\sqrt{s_{NN}} = 2.7$,3.3,3.8, and 4.3 GeV from JAM cascade (dotted lines), JAM mean-field mode (JAM/MF) (dashed lines), JAM with a first-order phase transition (JAM/1OPT) (solid lines) are compared to the data from the E895 Collaboration [68].

There is a weak EoS dependence on the kaons and pions $v_1$ that is always a negative slope. The difference between the kaon and antikaon $v_1$ is due to the difference of the cross section: the antikaon can form resonances with nucleons similarly to pion-nucleon scatterings, thus it has larger cross sections than kaon-nucleon collisions. This also explains the similarity of the antikaon $v_1$ to the pion $v_1$. We note that the small kaon-nucleon cross section produces smaller $v_1$ for positive kaons compared to protons and pions.

### B. Comparison to the data

In this section, we compare our results on the flows from different modes to the experimental data.

In Fig. 3, the rapidity dependence of the proton directed flows from different modes of the model are compared to the data [68] at AGS energies. The cascade mode always underestimates the slope of the directed flow, which indicates a lack of pressure generated by the cascade mode. The inclusion of the hadronic mean field generates more pressure and improves the description of the data. JAM/1OPT simulation predicts larger $v_1$ at $\sqrt{s_{NN}} = 2.7$ GeV than in the cascade mode, which is because the 1OPT EoS implemented in JAM has a repulsive mean field in the hadronic phase. While, as beam energy increases, the system hits the softest point and the slope of the proton-directed flow becomes negative as originally predicted by the hydrodynamical approach [8]. However, experimental data show a positive slope of protons, and do not support a first-order phase transition at AGS energies. As we will show in Fig. 16 elliptic flows at AGS energies support the hadronic mean-field approach as well, which predicts the suppressed elliptic flow.

However, as seen in Fig. 4, STAR data from RHIC-BES experiments at $\sqrt{s_{NN}} = 7.7$ GeV seems to be consistent with a 1OPT scenario in JAM rather than the result from JAM mean-field simulations: A first-order phase transition enhances

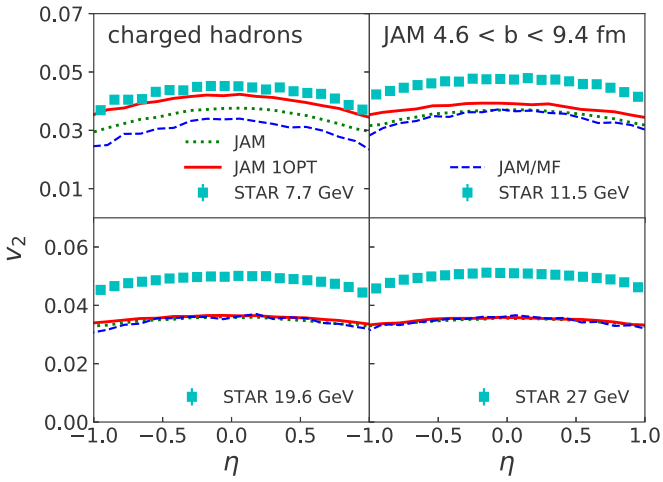


FIG. 4. Elliptic flows of charged hadrons as a function of rapidity in midcentral (10–40%) Au + Au collisions at $\sqrt{s_{NN}} =$ 7.7, 11.5, 19.6, and 27 GeV from JAM cascade (dotted lines), JAM with a fisrt-order phase transition (solid lines) are compared to the STAR data [69].

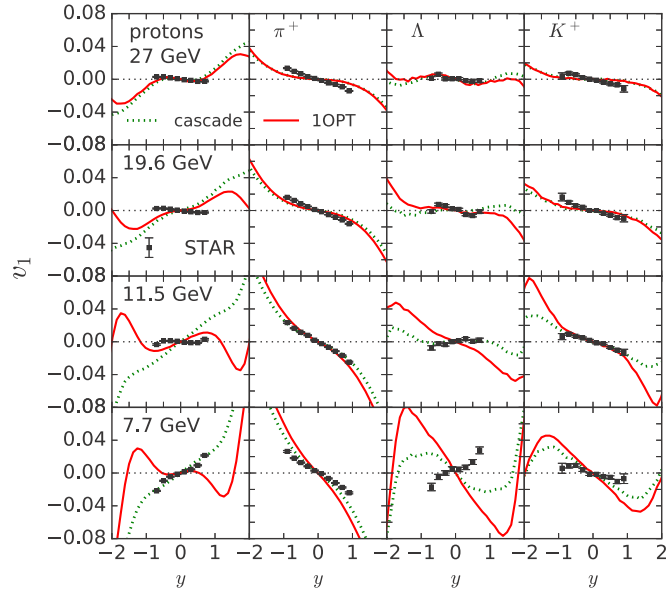


FIG. 5. Rapidity dependence of directed flow for protons, pions, Λs, and kaons in midcentral (10–40%) Au + Au collisions at $\sqrt{s_{NN}} =$ 7.7, 11.5, 19.6, and 27 GeV calculated with the JAM cascade (dotted lines) and the JAM with a first-order phase transition (solid lines) are compared to STAR data [33,70].

the elliptic flow, while the hadronic mean field suppresses the elliptic flow. At higher beam energies, all JAM simulations predict the same amount of elliptic flows, which is below the data. This may be due to the lack of a partonic degree of freedom in the model. It is reported that the experimentally observed increase of the elliptic flow with beam energy is reproduced by the inclusion of partonic interactions into microscopic transport model PHSD [71,72].

Recently, STAR measured directed flows of identified particles including Λs and kaons [70]. The measurements show that Λ directed flow exhibits the same behavior as protons, which cannot be accounted for within our model as seen in Fig. 5. JAM predicts a positive slope for protons, and negative slope for Λ below $\sqrt{s_{NN}} \leqslant 19.6$ GeV. As we will investigate in detail a generation mechanism of directed flow within our model, positive slope of proton-directed flow is generated by meson-baryon scatterings: initial nucleon-nucleon scatterings generate negative baryon directed flow. Initially generated negative proton flow changes its direction to the positive side by nucleon-pion scattering. However, as the Λ-meson scattering rate is very small, Λ-directed flow remains negative. Thus, dynamical models based on baryon and meson degrees of freedom hardly describe the similarly of the directed flow between protons and Λs. We may need a model that incorporates the effects of partonic interactions. One expects to get the similar directed flow of protons and Λs, if their are mainly generated in the partonic phase. Measurements of other baryons such as Ξ and Ω baryons may help to confirm the importance of the deconfined phase in the early stages of the reaction, if they also show similar behavior as protons in directed flows.

The directed flows of pions and kaons exhibits negative slopes for all beam energies, which is consistent with our model results. As we will study in detail the generation mechanisms of flows, the main source of the negative slopes of meson flows are the interaction with the spectator nucleons.

## IV. HADRONIC RESCATTERING AND SPECTATOR EFFECTS

Next we would like to investigate in detail the role of spectator interactions on the flows. As demonstrated in Ref. [47], the interplay between in- and out-of-plane flow plays an essential role to determine the final strength of the elliptic flow. To perform a detailed analysis of the effects of hadronic rescattering and spectator matter on anisotropic flows, we compute anisotropic flows by disabling meson-baryon ($MB$) and meson-meson ($MM$) scatterings; a simulation in which the cross sections of $MB$ and $MM$ scatterings are set to be zero. The effect of spectator shadowing is studied by disabling the interaction between spectator nucleons and participants, where spectator nucleons are defined in our approach as the nucleons that are not in the collision list of the initial state nucleon-nucleon collisions. More specifically, we first compute possible nucleon-nucleon collisions after sampling nucleons inside two nuclei and boost them, which corresponds to the initial Glauber-type nucleon-nucleon collisions. If nucleons in the projectile nucleus are considered not to collide with any other nucleons in the target nucleus, these nucleons are regarded as spectator nucleons, which are initially located outside a reaction zone of two nuclei. We assume that collision can happen when the impact parameter of the two incoming particles $b$ are inside the interaction distance specified by the geometrical interpolation of the cross section $\sigma$, i.e., $b \leqslant \sqrt{\sigma/\pi}$. Of course, if the beam energy is not very high, "spectator nucleons" can interact with nucleons in participant zone. In our simulations, we update the collision list after every two-body collision, thus the initially predicted nucleon-nucleon collision can be modified according to the dynamics of the collision of two nuclei.

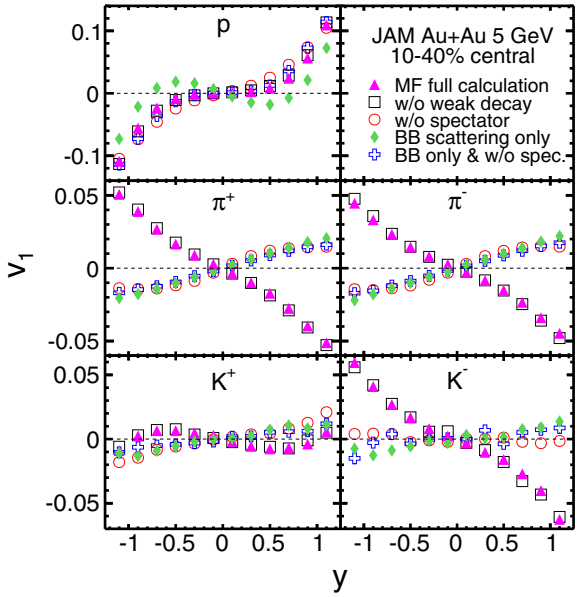


FIG. 6. Directed flows as a function of rapidity in midcentral (10–40%) Au + Au collision at $\sqrt{s_{NN}} = 5$ GeV from JAM mean-field mode (JAM/MF) (triangles), JAM/MF without weak decay (squires), JAM/MF without spectator (circles), JAM/MF with only baryon-baryon collisions (diamonds), and JAM/MF with only baryon-baryon collisions and without spectator (crosses). The left and right panels show the results for identified particles $p$, $\pi^+$, $K^+$ and antiparticles $\pi^-$, $K^-$, respectively.

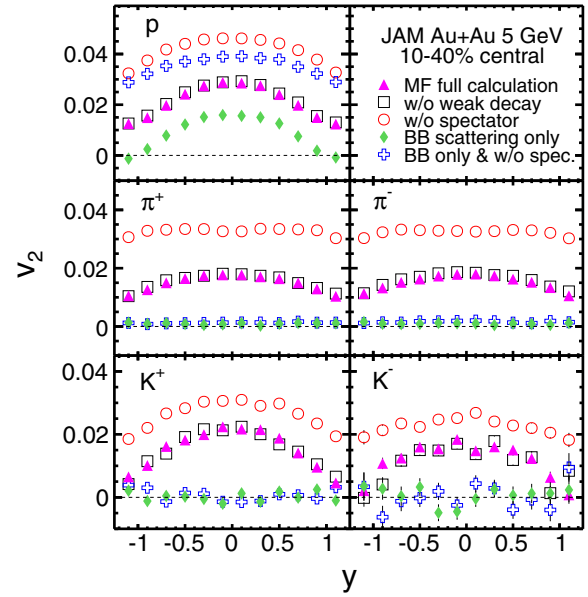


FIG. 7. Same as Fig. 6, but for $v_2$.

### A. Directed flow

Figure 6 shows the rapidity dependence of directed flow for identified particles ($p$, $\pi^+$, $K^+$) and corresponding antiparticles ($\pi^-$, $K^-$) in midcentral (10–40%) Au + Au collision at $\sqrt{s_{NN}} = 5$ GeV from JAM mean-field (JAM/MF) simulations. JAM/MF simulation predicts positive $v_1$ for protons and negative $v_1$ for pions and kaons. To see the effect of $MB$ and $MM$ scattering, we show the results of simulation by switching off $MB$ and $MM$ scatterings, i.e., baryon-baryon ($BB$) collision only (diamonds) simulations, which yield negative $v_1$ for protons and positive $v_1$ for pions and kaons. We also test the effects of spectator matter by disabling the interaction with spectator [without spectator (circles)]. This simulation shows that nucleon $v_1$ is positive and larger at midrapidity compared to the full simulations. The pion and kaon $v_1$ are also positive with this simulation. If we disable both interaction with spectator and meson-baryon scatterings, nucleon $v_1$ becomes almost zero at midrapidity. Thus, it is clear that the negative nucleon $v_1$ in the $BB$ scattering only simulation is due to the shadowing effect by the spectator matter, whereas meson-baryon collisions reflect nucleons to the positive $v_1$ and pions to the negative side. It is also demonstrated that *all* of the negative $v_1$ for pions are generated by the interaction between spectator nucleons and pions.

We also studied the effects of weak decays since some nucleons and pions are produced from the weak decay such as $\Lambda^0$, and $\Sigma^-$, and this may affect the distribution of flows. We observe that directed flow is not sensitive to the weak decay effects at 5 GeV.

### B. Elliptic flow

We do the same excises for elliptic flow. In Fig. 7, the rapidity dependence of $v_2$ for identified particles ($p$, $\pi^+$, $K^+$) and corresponding antiparticles ($\pi^-$, $K^-$) in midcentral Au + Au collisions at $\sqrt{s_{NN}} = 5$ GeV from the JAM mean-field mode are presented. Elliptic flow is generated by the scattering among hadrons in JAM. When $MB$ and $MM$ scatterings are disabled, nucleon $v_2$ are smaller by about 20%, and pion and kaon elliptic flows are zero. It is seen that the effect of spectator on the elliptic flow is very large for entire rapidity range at 5 GeV for all particles. The spectator effects on the elliptic flow for nucleons and pions are 20–40% reduction at $\sqrt{s_{NN}} = 5$ GeV at midrapidity. The shape of the rapidity distribution is mainly determined by the degree of suppression of the elliptic flow.

Collision centrality dependence may also contain important information about the collision dynamics in heavy-ion collisions. Figures 8 and 9 display the centrality dependence of integrated $v_2$ for particles ($p$, $\pi^+$, $K^+$, $\pi^-$, $K^-$) and charged hadrons from JAM mean-field simulations in Au + Au collisions at $\sqrt{s_{NN}} = 5$ GeV. The suppression of the elliptic flow by the spectator can be seen for all centrality for all particles except for very central collisions. It is interesting to see that elliptic flow becomes negative at very peripheral collisions even at 5 GeV.

### C. Squeeze-out and softening

In this section, we discuss the squeeze-out effect on the elliptic flow when a softening of EoS happens. In Refs. [46,47], it was found that the softening of EoS leads to an enhancement of elliptic flow, which is considered to be caused by the suppression of squeeze-out at high baryon density region, and proposed as a possible signature of a first-order phase transition. Attractive orbit simulation shows the enhancement of $v_2$ for pions [46], whereas a simulation with a first-order

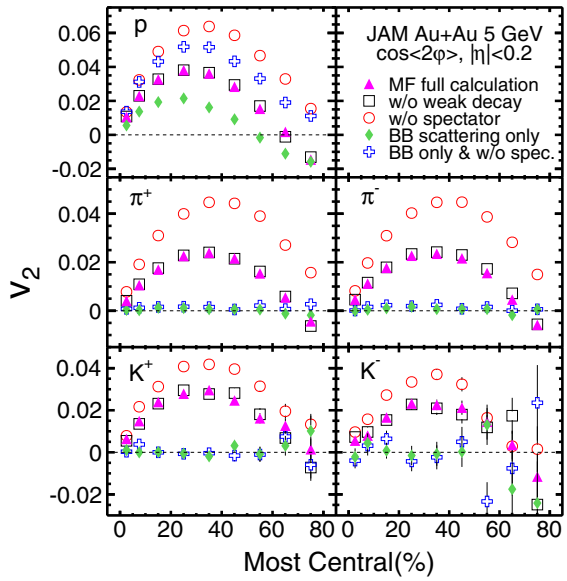


FIG. 8. Same as Fig. 7, but for the centrality dependence of the $\eta$ integrated $v_2$ at $|\eta| < 0.2$.

phase transition predicts enhancement of $v_2$ for both protons and pions [47]. Here we shall see explicitly that the softening indeed suppresses the squeeze-out.

To understand the role of squeeze-out in the case of softening more qualitatively, the elliptic flow from attractive orbit simulation is compared to the standard JAM cascade simulation with and without spectator in Fig. 10. Without spectator interaction, attractive orbit simulation yields less nucleon $v_2$ than from standard cascade simulation. This is because attractive orbit simulation leads to very small pressure for all space-time regions of the reaction. However, the situation changes in the case of the presence of a spectator. It blocks the in-plane expansion at early times and suppresses $v_2$. The degree of suppression is weaker in the case of softening. We observe that the effect of squeeze-out becomes less in the case of softening: a reduction of nucleon $v_2$ in the cascade mode is about 30%, while there is almost no reduction in the attractive orbit mode.

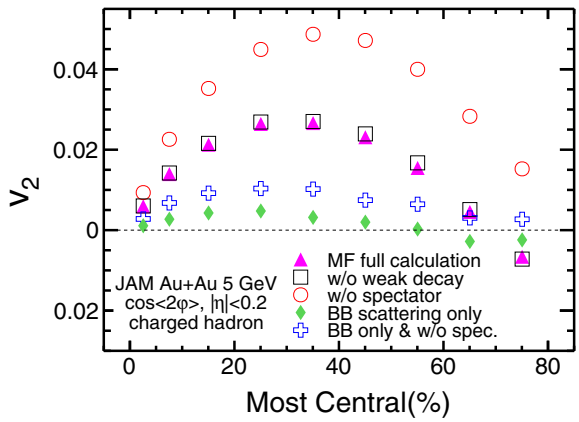


FIG. 9. Same as Fig. 8 but for charged particles.

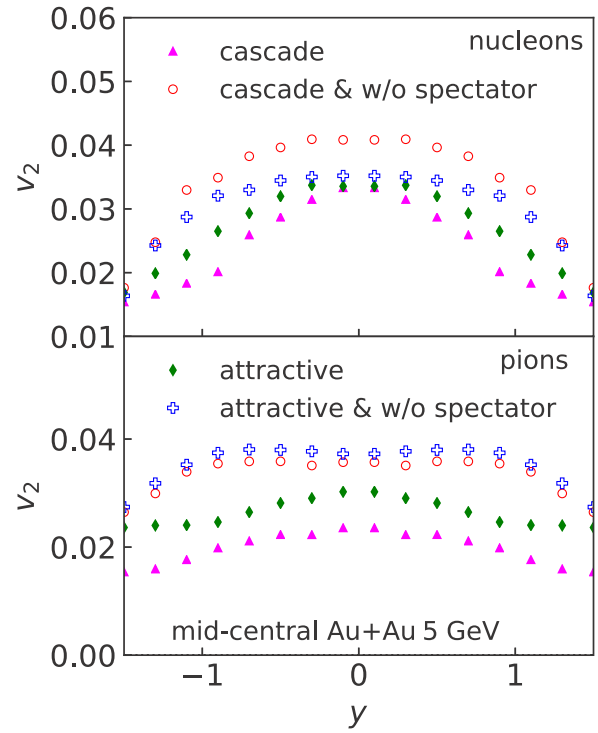


FIG. 10. Rapidity dependence of $v_2$ for nucleons (upper) and pions (lower) in midcentral Au + Au at $\sqrt{s_{NN}} = 5$ GeV are compared to the JAM cascade and JAM attractive orbit mode with and without spectator interaction.

In the case of pions, $v_2$ in the attractive orbit simulation is almost the same as that of the cascade simulation without interaction with the spectator matter. It is seen that pion $v_2$ are suppressed more by the spectator for the cascade simulation. The net effect is a larger $v_2$ in the attractive mode compared to the cascade mode.

Attractive orbit simulation strongly suppresses the pressure of the system for whole reaction time and all spatial regions of the system regardless of its energy density since we force the attractive orbit for all two-body scatterings without any restrictions, which is considered to be a maximum effect of softening within our approach. To take into account the softening effect only if the system enters the softening point, we perform a simulation with a 1OPT [32], and the results are shown in Fig. 11. The elliptic flow in the 1OPT simulation without spectator becomes larger than the cascade results. This may be because the system is compressed more in the 1OPT simulation, and as shown in Ref. [47], the initial eccentricity becomes larger, but during the expansion, the system eventually goes out from the soft region and generates stronger in-plane flow. We also note that nucleon elliptic flow is not suppressed by the spectator shadowing at midrapidity in the case of 1OPT as well, while pion elliptic flow is suppressed by the spectator even in the 1OPT for pions, although the degree of suppression is less.

This analysis indicates that the final value of the elliptic flow at high baryon density region is determined by the interplay between in-plane and out-of-plane emission, and it is very sensitive to the pressure of the system.

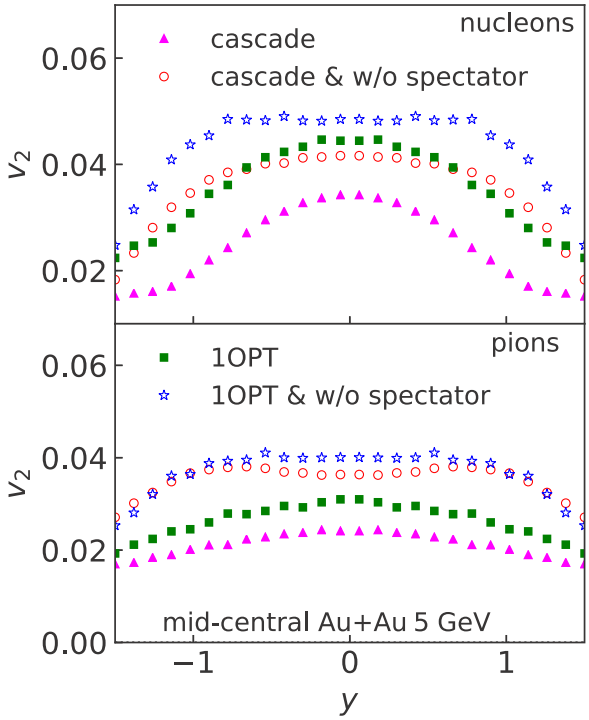


FIG. 11. Rapidity dependence of $v_2$ for nucleons (upper) and pions (lower) in midcentral Au + Au at $\sqrt{s_{NN}} = 5$ GeV are compared to the JAM cascade and JAM first-order phase transition mode with and without spectator interaction.

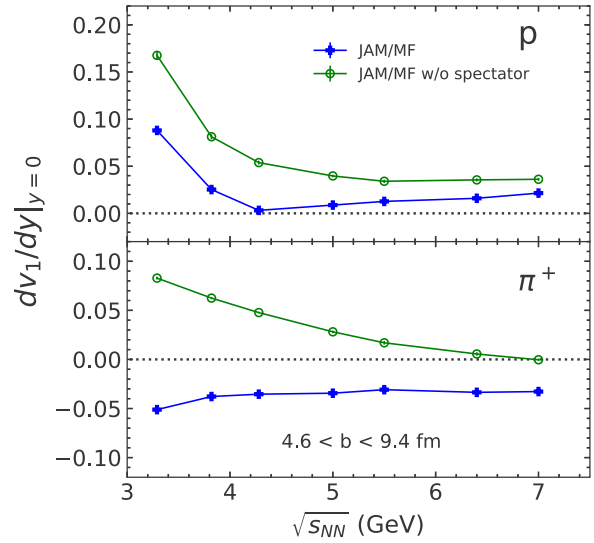


FIG. 12. Beam energy dependence of the slope of directed flow in midcentral (10–40%) Au + Au collision from JAM mean-field mode (MF) (crosses), and MF without spectator (circles). Slope $dv_1/dy$ is obtained by the cubic fit at the range of $|y| < 0.8$. The top and bottom panels show the results for protons and positive pions, respectively.

## V. BEAM ENERGY DEPENDENCE

The beam energy dependence of the spectator effects will be investigated in this section. At sufficiently high energies such as at top RHIC and LHC energies, the hybridization of reaction dynamics is successful in describing the collision of high-energy heavy-ion collisions. One of them is the "factorization" of reaction time in which heavy-ion collision can be separated by the initial Glauber-type nucleon-nucleon collisions that provides the initial conditions for the subsequent space-time evolution of the system by, e.g., hydrodynamics or transport theories. One may estimate the minimum beam energy at which this factorization of reaction time becomes applicable by considering a passing time of two nuclei.

The passing time of two nuclei $t_{\rm pass}$ can be estimated by using the radius $R$, velocity $v$ of the nucleus, and $\gamma$ factor as $t_{\rm pass} = 2R/\gamma/v \approx 0.9\,{\rm fm}/c$ at 27 GeV. Thus we expect that collision dynamics changes around this beam energy, assuming that the typical formation time of the produced particle is about 1 fm/$c$. Above this energy, the initial condition for a subsequent evolution of the system can be obtained by the initial particle production just after the collision of two nuclei, which may be computed by the Glauber model or theories based on the color glass condensate (CGC) [2,73–75]. On the other hand, below this beam energies, this factorization breaks down and we need to take into account the rescatterings of particles during the passage of two nuclei. A new dynamical initialization is proposed in the hydrodynamical approach to simulate lower beam energies in Ref. [76] taking into account such effects. If rescatterings among produced particles happen during the passage of two nuclei, interactions with the spectator nucleons become also important in the early stages of heavy-ion collision, and it has a significant impact on the anisotropic flows.

When we go down to even lower beam energies such as $\sqrt{s_{NN}} \lesssim 5$ GeV, nuclear mean-field effects become important, and microscopic transport approaches based on the Boltzmann-Uehling-Uhlenbeack (BUU) equation [77] or the quantum molecular dynamics (QMD) $N$-body phase-space dynamics [78] have been successful in describing collision dynamics. We shall study the transition of generation mechanisms of anisotropic flows within a microscopic transport approach below.

### A. AGS energies

We first investigate beam energy dependence at AGS energies where nuclear mean-field effects play an important role. In Fig. 12, the beam energy dependence of the slopes of directed flow $dv_1/dy$ at midrapidity are shown for protons and positive pions from JAM with the mean-field simulations. The $v_1$ slope at midrapidity without spectator interaction is larger compared to the full calculations. Thus, it demonstrates that the directed flow at midrapidity is significantly influenced by the shadowing effect by the spectator even at midrapidity. At higher beam energies, as we shall investigate in the next section, the shadowing effect by the spectator is not seen for the nucleon $v_1$ slope because of the increasing number of scatterings between pions and nucleons. The $v_1$ slopes for pions are negative in the full simulations, while they are positive without spectator interactions. Thus, negative-directed flow for pions is generated solely by the interaction with the spectator in this beam energy range.

In Fig. 13, the beam energy dependence of the elliptic flows of protons and positive pions at midrapidity $v_2(|y| < 0.2)$ is shown. Without spectator interaction, the elliptic flow

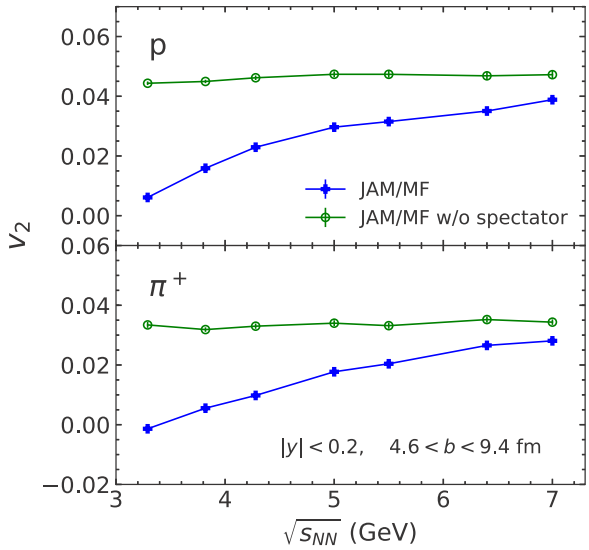


FIG. 13. Same as Fig. 12, but for beam energy dependence of elliptic flows $v_2$ at midrapidity $|y| < 0.2$.

excitation function is almost flat for both protons and pions at beam energies $3 < \sqrt{s_{NN}} < 7$ GeV which indicates that elliptic flow at midrapidity in this energy region is mainly determined by the degree of shadowing by the spectator. The relative contribution of the squeeze-out effect to the elliptic flow decreases smoothly as the beam energy increases: the out-of-plane flow (squeeze-out) is large in the beam energy $\sqrt{s_{NN}} < 4$ GeV, while both out-of-plane and in-plane contributions are important at $5 < \sqrt{s_{NN}} < 6$, and then, in-plane flow becomes dominant at $\sqrt{s_{NN}} > 6.5$ GeV.

### B. RHIC-BES energies

We now study the beam energy dependence of the effects of rescattering and spectator shadowing for directed and elliptic flows at RHIC-BES energy region.

#### *1. Directed flow*

Figure 14 shows the beam energy dependence of directed flow as a function of rapidity for nucleons (left panel) and pions (right panel) from 6.4 to 62.4 GeV obtained by the cascade mode. One may refer to Refs. [31,60] for the comparison to the STAR data at midrapidity with different EoS. Here we focus on the rapidity dependence on the flows up to the beam rapidity region.

Let us first compare the simulation without rescattering; i.e., simulations that include only $BB$ collisions. The shadowing effect by the spectator can be seen in the $BB$ only simulations up to 19.6 GeV. Namely, the slope of the nucleon-directed flow is negative when $MB$ and $MM$ scatterings are disabled (dotted-dashed lines), while it is almost zero if there are only $BB$ scatterings and there is no spectator (dotted lines). This implies that nucleon-directed flow is negative due to the shadowing effect by the spectator when only $BB$ collisions are included. Once $MB$ and $MM$ scatterings are turned on, slope becomes positive, and the shadowing effect is washed out: the directed flow of nucleon $v_1$ at $y/y_{\rm c.m.} < 0.75$ in the

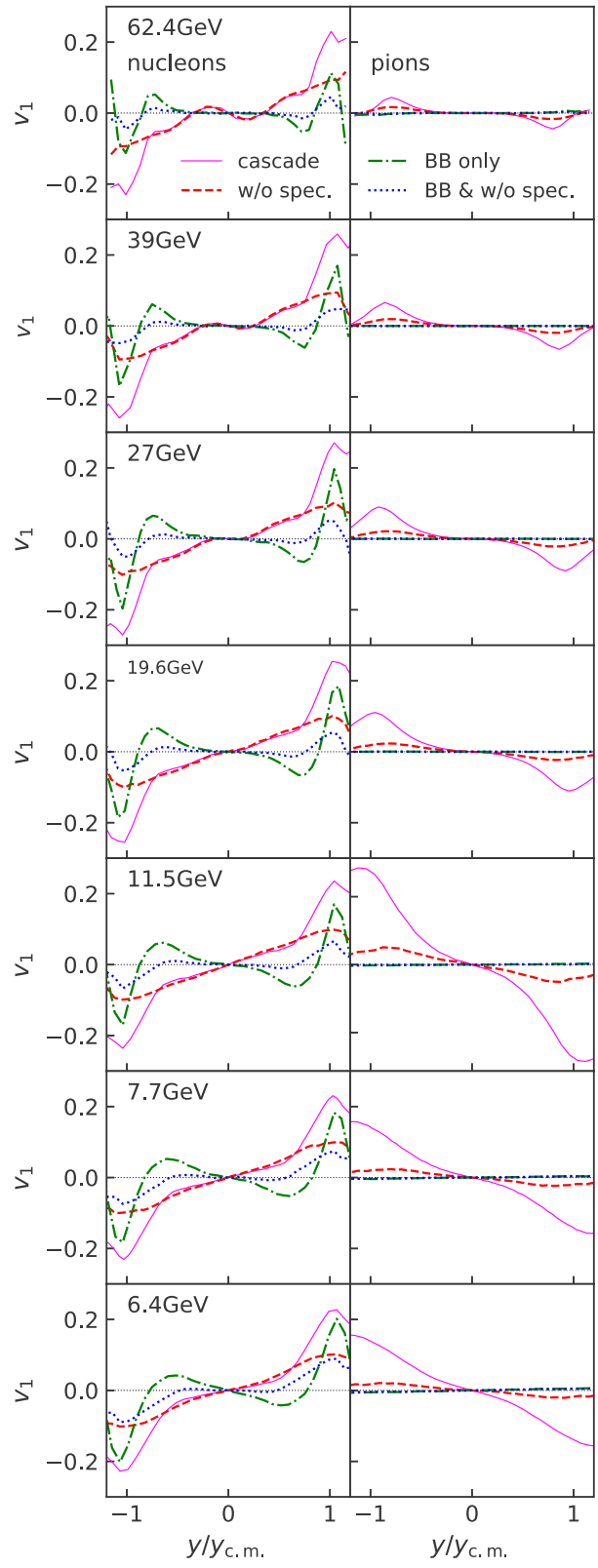


FIG. 14. Rapidity dependence of directed flow for nucleons (left panel) and pions (right panel) are compared in midcentral Au + Au collisions ($4.6 < b < 9.6$ fm) at $\sqrt{s_{NN}} = 6.4$, 7.7, 11.5, 19.6, 27, 39 and 62.4 GeV from JAM cascade simulations. In the calculations, acceptance cut $0.4 \leqslant p_T \leqslant 2\,\text{GeV}/c$ for nucleons, $0.2 \leqslant p_T \leqslant 1.6\,\text{GeV}/c$ for pions are imposed.

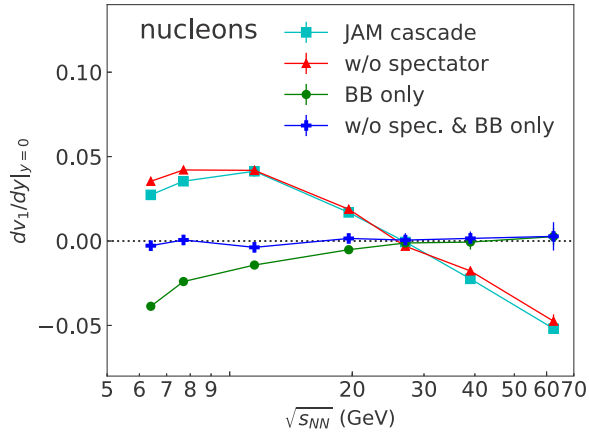


FIG. 15. Beam dependence of the slope of nucleon directed flow in midcentral (10–40%) Au + Au collision from JAM cascade (squires), cascade without spectator (triangles), cascade with only baryon-baryon collisions (circles), and cascade with only baryon-baryon collisions and without spectator (crosses).

full cascade simulation with spectator (solid lines) is almost identical to the results of the simulations without spectator interaction (dashed lines). Thus the shadowing effect on the directed flow of nucleons is not seen in the final strength of the directed flow at the rapidity region of $y/y_{\text{c.m.}} < 0.75$. In contrast, most of the pion-directed flow is generated by the interaction with the spectator matter.

When the beam energy becomes higher than 20 GeV, the collision dynamics changes dramatically, as expected from the passing time argument. The slope of the nucleon-directed flow at midrapidity becomes negative from 27 GeV in the full cascade simulations, as predicted by Ref. [35] and called wiggle shape. It is explained [35] by the space-momentum correlation and the degree of baryon stopping, which is not a shadowing effect by the spectator matter. This is confirmed by the results that the $BB$ only simulation yields the same results when interaction with the spectator matter is turned off: the nucleon-directed flow is almost zero for both $BB$ only simulation and $BB$ only without spectator simulation at high energies. In our hadronic transport approach, the space-momentum correlation is generated by rescattering among particles after two nuclei pass through each other at high energies above 30 GeV, thus $MB$ scattering generates a negative nucleon-directed flow at high energies. It is shown that the tilted initial condition yields the negative $v_1$ slope in hydrodynamics at RHIC [79]. We note that CGC also predicts tilted initial conditions [80].

It is interesting to observe that at the forward rapidity region $y/y_{\text{c.m.}} > 0.75$, the directed flow of the nucleon looks identical for all beam energies suggesting the universal mechanism to generate the directed flow at forward rapidity regions. At high energies, the pion-directed flow at the forward rapidity region is also generated by the spectator shadowing.

To see more clearly the different mechanisms for the origin of the directed flow of nucleons at midrapidity, the slopes of nucleon $v_1$ are depicted in Fig. 15 as a function of beam energy, where the slope is obtained by the linear fit at $|y| < 0.5$. If both the spectator interaction and $MB$ and $MM$ scatterings

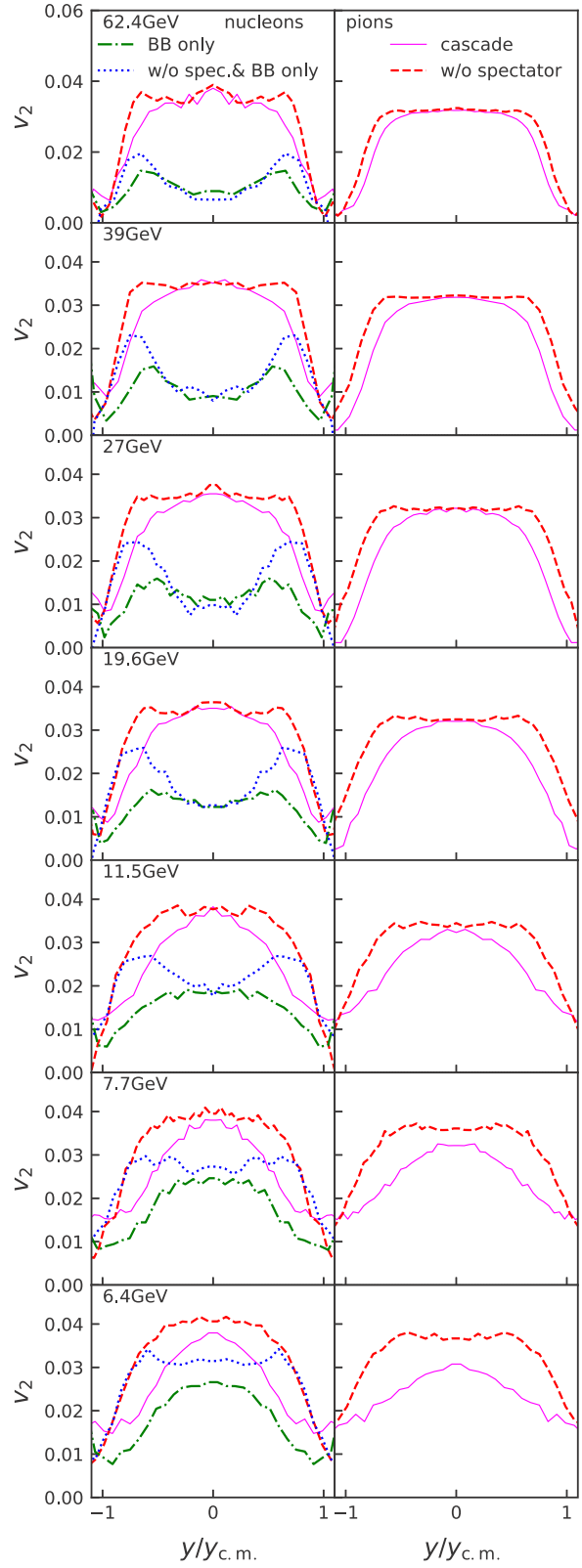


FIG. 16. Rapidity dependence of $v_2$ for nucleons (left panel) and pions (right panel) are compared in midcentral Au + Au collisions ($4.6 < b < 9.6$ fm) at $\sqrt{s_{NN}} = 6.4$, 7.7, 11.5, 19.6, 27, 39 and 62.4 GeV from JAM cascade simulations. In the calculations, acceptance cut $0.4 \leqslant p_T \leqslant 2\,\text{GeV}/c$ for nucleons, $0.2 \leqslant p_T \leqslant 1.6\,\text{GeV}/c$ for pions are imposed.

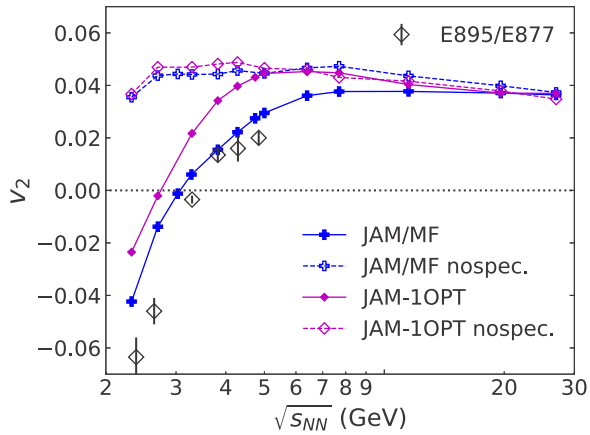


FIG. 17. Beam energy dependence of $v_2$ for nucleons in midcentral Au + Au collisions ($4.6 < b < 9.4$ fm) from JAM first-order phase transition and mean-field simulations with and without spectator interactions. Data are take from Ref. [84].

are disabled, the directed flow is not generated (crosses). Once interaction with the spectator is included, $BB$ collisions generate negative-directed flow as a result of the shadowing up to the beam energy of around 30 GeV, while above 30 GeV, the $BB$ collision does not generate directed flow even with the spectator. Thus there is no effect of spectator shadowing on the directed flow of the nucleon at midrapidity above 30 GeV. The role of final state interactions (mostly $MB$ and $MM$ scattering in our case) to the slope of nucleon-directed flow is opposite at low and high energies. Namely, the effect of $MB$ and $MM$ collisions is to generate positive nucleon directed flow below 30 GeV, while they generate negative-directed flow above 30 GeV. Thus the dynamical origin of directed flow changes at 30 GeV.

#### 2. *Elliptic flow*

In Fig. 16, the rapidity dependence of the elliptic flow for nucleons and pions are plotted for the beam energy range of $6.4 \leqslant \sqrt{s_{NN}} \leqslant 62.4$ GeV in midcentral Au + Au collisions. It is seen by comparing the result of the JAM cascade (solid line) with the simulation without spectator interaction (dashed line) that at lower energies $\sqrt{s_{NN}} \leqslant 7.7$ GeV, the suppression of the elliptic flow by the spectator matter is large for all rapidity regions for both nucleons and pions. The contribution of $MB$ and $MM$ scatterings to the elliptic flow is increasingly significant as the beam energy increases. The spectator effect on the elliptic flow at midrapidity disappears at above 11.5 GeV, but the suppression of the elliptic flow is still seen at $y/y_{\rm c.m.} > 0.5$, which becomes smaller as the beam energy increases. At higher beam energies, the elliptic flow for both nucleons and pions becomes flat in the hadronic cascade simulation. It was reported that at the forward rapidity region, the elliptic flow from hadronic transport models is consistent with the RHIC data [81]. However, three-dimensional-hydrodynamics supplemented by a hadron transport afterburner also predicts a compatible amount of elliptic flow at forward rapidities [82,83]. Our results demonstrate that the interaction with the spectator plays a minor role for the generation of elliptic flow for a wide range of rapidity region at sufficiently higher energies.

Figure 17 summarizes the effect of spectator shadowing on the elliptic flow of nucleons at midrapidity as a function of beam energy for mean-field simulation as well as simulations with a first-order phase transition. The repulsive potential generates more pressures, as a result there is a spectator shadowing up to the beam energy of 10 GeV. On the other hand, the spectator shadowing disappears due to the strong softening effect in a first-order phase transition around 5 GeV, and calculations with and without spectator interaction show almost identical results at $\sqrt{s_{NN}} > 5$ GeV. Measurements of the elliptic flow at the beam energy range of $5 < \sqrt{s_{NN}} < 10$ GeV, which is being planed at FAIR, NICA, and J-PARC-HI, help to extract an important information on the pressure of the dense baryonic system created in heavy-ion collisions.

## VI. SUMMARY

We study the role of meson-baryon and meson-meson rescattering as well as the interaction with spectator matter on the generation of directed and elliptic flows including EoS dependence in Au + Au collisions at $2.3 \leqslant \sqrt{s_{NN}} \leqslant 62.4$ GeV. It is found that initial nucleon-nucleon collisions during the passage of two-nuclei (Glauber-type scattering) generate negative nucleon-directed flow at the beam energy up to 27 GeV due to the spectator shadowing, but above 27 GeV its effect becomes negligible at midrapidity. $BM$ and $MM$ scatterings generate positive nucleon-directed flow below 27 GeV, while they generate negative nucleon flow above 27 GeV. The main difference in the collision dynamics below and above 27 GeV is that rescattering happens during the passage of two nuclei below 27 GeV, while rescatterings start after the passage of two nuclei above 27 GeV (after making tilted initial condition). Universal behavior of the nucleon directed flow at the forward rapidity region $y > 0.75 y_{\rm c.m.}$ is observed. Pion-directed flow is the result of the interaction between pion and spectator nucleons, which generate negative-directed flow for all beam energies investigated in this work.

Our study demonstrates the importance of spectator interaction on directed and elliptic flows in Au + Au collisions at high baryon density region $\sqrt{s_{NN}} < 10$ GeV for all rapidity ranges. The squeeze-out effect by the spectator to the elliptic flow becomes negligible at midrapidity at above 10 GeV. The degree of shadowing by the spectator matter decreases as the beam energy increases at the forward rapidity region, and its effect becomes very small at 62.4 GeV, thus it supports some hydrodynamical approaches that do not include spectators in the calculations. Finally, we show that the enhancement of the elliptic flow by the softening of EoS is largely due to the absence of the squeeze-out effect at $5 < \sqrt{s_{NN}} < 10$ GeV. As a future study, the systematic investigation of collision system dependence is planned.

## ACKNOWLEDGMENTS

This work is supported by the MoST of China 973-Project No. 2015CB856901, NSFC under Grant Nos. 11575069 and 11521064. Y.N. is supported by the Grants-in-Aid for Scientific Research from JSPS (Nos. JP15K05079, JP15K05098, and JP17K05448).

[1] Arsene *et al.* (BRAHMS Collaboration), Nucl. Phys. A **757**, 1 (2005); B. B. Back *et al.* (STAR Collaboration), *ibid.* **757**, 102 (2005); K. Adcox *et al.* (PHENIX Collaboration), *ibid.* **757**, 184 (2005).

[2] U. Heinz and R. Snellings, Ann. Rev. Nucl. Part. Sci. **63**, 123 (2013).

[3] W. Busza, K. Rajagopal, and W. van der Schee, arXiv:1802.04801.

[4] Y. Aoki, G. Endrodi, Z. Fodor, S. D. Katz, and K. K. Szabo, Nature **443**, 675 (2006).

[5] B. Friman, C. Hohne, J. Knoll, S. Leupold, J. Randrup, R. Rapp, and P. Senger, Lect. Notes Phys. **814**, 1 (2011).

[6] M. Asakawa and K. Yazaki, Nucl. Phys. A **504**, 668 (1989); D. H. Rischke, Prog. Part. Nucl. Phys. **52**, 197 (2004); M. A. Stephanov, Prog. Theor. Phys. Suppl. **153**, 139 (2004); Int. J. Mod. Phys. A **20**, 4387 (2005); K. Fukushima and C. Sasaki, Prog. Part. Nucl. Phys. **72**, 99 (2013).

[7] C. M. Hung and E. V. Shuryak, Phys. Rev. Lett. **75**, 4003 (1995).

[8] D. H. Rischke, Y. Pürsün, J. A. Maruhn, H. Stöcker, and W. Greiner, Acta Phys. Hung. A **1**, 309 (1995).

[9] S. Gupta, X. Luo, B. Mohanty, H. G. Ritter, and N. Xu, Science **332**, 1525 (2011).

[10] L. Kumar, Mod. Phys. Lett. A **28**, 1330033 (2013).

[11] X. Luo and N. Xu, Nucl. Sci. Tech. **28**, 112 (2017).

[12] G. Odyniec, Euro. Phys. J Web Conf. **95**, 03027 (2015).

[13] C. Hhne (CBM Collaboration), J. Phys. Conf. Ser. **420**, 012016 (2013).

[14] T. Ablyazimov *et al.* (CBM Collaboration), Eur. Phys. J. A **53**, 60 (2017).

[15] H. Sako *et al.* (J-PARC Heavy-Ion Collaboration), Nucl. Phys. A **931**, 1158 (2014); H. Sako, *ibid.* **956**, 850 (2016).

[16] L. Turko (NA61/SHINE Collaboration), Universe **4**, 52 (2018).

[17] V. Kekelidze, A. Kovalenko, R. Lednicky, V. Matveev, I. Meshkov, A. Sorin, and G. Trubnikov, Nucl. Phys. A **956**, 846 (2016).

[18] J. Hofmann, H. Stoecker, U. W. Heinz, W. Scheid, and W. Greiner, Phys. Rev. Lett. **36**, 88 (1976).

[19] H. Stoecker and W. Greiner, Phys. Rept. **137**, 277 (1986).

[20] H. Stoecker, Nucl. Phys. A **750**, 121 (2005).

[21] H. G. Baumgardt, J. U. Schott, Y. Sakamoto. E. Schopper, H. Stoecker, J. Hofmann, W. Scheid, and W. Greiner, Z. Phys. A **273**, 359 (1975).

[22] S. Voloshin and Y. Zhang, Z. Phys. C **70**, 665 (1996).

[23] A. M. Poskanzer and S. A. Voloshin, Phys. Rev. C **58**, 1671 (1998).

[24] S. A. Voloshin, A. M. Poskanzer, and R. Snellings, in *Relativistic Heavy Ion Physics* (Springer, New York, 2010), pp. 293–333.

[25] J. Brachmann, S. Soff, A. Dumitru, H. Stöcker, J. A. Maruhn, W. Greiner, L. V. Bravina, and D. H. Rischke, Phys. Rev. C **61**, 024909 (2000).

[26] Y. B. Ivanov, E. G. Nikonov, W. Noerenberg, A. A. Shanenko, and V. D. Toneev, Acta Phys. Hung. A **15**, 117 (2002).

[27] J. Brachmann, A. Dumitru, H. Stoecker, and W. Greiner, Eur. Phys. J. A **8**, 549 (2000).

[28] L. P. Csernai and D. Rohrich, Phys. Lett. B **458**, 454 (1999).

[29] L. P. Csernai, A. Anderlik, C. Anderlik, V. K. Magas, E. Molnar, A. Nyiri, D. Rohrich, and K. Tamosiunas, Acta Phys. Hung. A **22**, 181 (2005).

[30] J. Steinheimer, J. Auvinen, H. Petersen, M. Bleicher, and H. Stöcker, Phys. Rev. C **89**, 054913 (2014).

[31] Y. Nara, H. Niemi, A. Ohnishi, and H. Stöcker, Phys. Rev. C **94**, 034906 (2016).

[32] Y. Nara, H. Niemi, J. Steinheimer, and H. Stöcker, Phys. Lett. B **769**, 543 (2017).

[33] L. Adamczyk *et al.* (STAR Collaborations), Phys. Rev. Lett. **112**, 162301 (2014).

[34] P. Shanmuganathan (STAR Collaboration), Nucl. Phys. A **956**, 260 (2016).

[35] R. J. M. Snellings, H. Sorge, S. A. Voloshin, F. Q. Wang, and N. Xu, Phys. Rev. Lett. B **84**, 2803 (2000).

[36] M. Bleicher and H. Stoecker, Phys. Lett. B **526**, 309 (2002).

[37] V. P. Konchakovski, W. Cassing, Y. B. Ivanov, and V. D. Toneev, Phys. Rev. C. **90**, 014903 (2014).

[38] H. Petersen, Q. Li, X. Zhu, and M. Bleicher, Phys. Rev. C **74**, 064908 (2006).

[39] H. Sorge, Phys. Rev. Lett. **78**, 2309 (1997).

[40] D. Teaney, J. Lauret, and E. V. Shuryak, Phys. Rev. Lett. **86**, 4783 (2001).

[41] U. Heinz, Nucl. Phys. A **830**, 287 (2009).

[42] H. Sorge, Phys. Rev. Lett. **82**, 2048 (1999).

[43] S. A. Bass, R. Mattiello, H. Stoecker, W. Greiner, and C. Hartnack, Phys. Lett. B **302**, 381 (1993).

[44] S. A. Bass, C. Hartnack, H. Stöcker, and W. Greiner, Phys. Rev. Lett. **71**, 1144 (1993).

[45] C. Hartnack, J. Aichelin, H. Stoecker, and W. Greiner, Phys. Lett. B **336**, 131 (1994).

[46] J. Chen, X. Luo, F. Liu, and Y. Nara, Chin. Phys. C **42**, 024001 (2018).

[47] Y. Nara, H. Niemi, A. Ohnishi, J. Steinheimer, X. Luo, and H. Stöcker, Eur. Phys. J. A **54**, 18 (2018).

[48] Y. Nara, N. Otuka, A. Ohnishi, K. Niita, and S. Chiba, Phys. Rev. C **61**, 024901 (1999).

[49] H. Sorge, Phys. Rev. C **52**, 3291 (1995); Phys. Lett. B **402**, 251 (1997).

[50] S. A. Bass *et al.*, Prog. Part. Nucl. Phys. **41**, 255 (1998).

[51] M. Bleicher *et al.*, J. Phys. G. **25**, 1859 (1999).

[52] Z.-W. Lin, C. M. Ko, B.-A. Li, B. Zhang, and S. Pal, Phys. Rev. C **72**, 064901 (2005).

[53] W. Cassing and E. L. Bratkovskaya, Nucl. Phys. A. **831**, 215 (2009).

[54] T. Hirano and Y. Nara, Prog. Theoret. Exper. Phys. **2012**, 01A203 (2012).

[55] T. Maruyama, K. Niita, T. Maruyama, S. Chiba, Y. Nakahara, and A. Iwamoto, Prog. Theor. Phys. **96**, 263 (1996).

[56] D. Mancusi, K. Niita, T. Maruyama, and L. Sihver, Phys. Rev. C **79**, 014614 (2009).

[57] H. Sorge, H. Stoecker, and W. Greiner, Annals Phys. **192**, 266 (1989).

[58] C. Gale, G. Bertsch, and S. Das Gupta, Phys. Rev. C **35**, 1666 (1987).

[59] M. Isse, A. Ohnishi, N. Otuka, P. K. Sahu, and Y. Nara, Phys. Rev. C **72**, 064908 (2005).

[60] Y. Nara and A. Ohnishi, Nucl. Phys. A **956**, 284 (2016).

[61] P. Danielewicz and S. Pratt, Phys. Rev. C **53**, 249 (1996).

[62] E. C. Halbert, Phys. Rev. C **23**, 295 (1981).

[63] M. Gyulassy, K. A. Frankel, and H. Stöcker, Phys. Lett. B **110**, 185 (1982).

[64] D. E. Kahana, D. Keane, Y. Pang, T. Schlagel, and S. Wang, Phys. Rev. Lett. **74**, 4404 (1995); D. E. Kahana, Y. Pang, and E. V. Shuryak, Phys. Rev. C **56**, 481 (1997).
[65] H. Petersen, J. Steinheimer, M. Bleicher, and H. Stoecker, J. Phys. G **36**, 055104 (2009).
[66] Y. B. Ivanov, Phys. Rev. C **89**, 024903 (2014).
[67] Y. B. Ivanov and A. A. Soldatov, Eur. Phys. J. A **52**, 10 (2016).
[68] H. Liu *et al.* (E895 Collaboration), Phys. Rev. Lett. **84**, 5488 (2000).
[69] L. Adamczyk *et al.* (STAR Collaboration), Phys. Rev. C **86**, 054908 (2012).
[70] L. Adamczyk *et al.* (STAR Collaboration), Phys. Rev. Lett. **120**, 062301 (2018).
[71] V. P. Konchakovski, E. L. Bratkovskaya, W. Cassing, V. D. Toneev, and V. Voronyuk, Phys. Rev. C **85**, 011902 (2012).
[72] V. P. Konchakovski, E. L. Bratkovskaya, W. Cassing, V. D. Toneev, S. A. Voloshin, and V. Voronyuk, Phys. Rev. C **85**, 044922 (2012).
[73] C. Gale, S. Jeon, and B. Schenke, Int. J. Mod. Phys. A **28**, 1340011 (2013).
[74] T. Hirano and Y. Nara, Nucl. Phys. A **743**, 305 (2004).
[75] T. Hirano, P. Huovinen, K. Murase, and Y. Nara, Prog. Part. Nucl. Phys. **70**, 108 (2013).
[76] C. Shen and B. Schenke, Phys. Rev. C **97**, 024907 (2018).
[77] G. F. Bertsch, H. Kruse, and S. Das Gupta, Phys. Rev. C **29**, 673, (1984); **33**, 1107(E) (1986); G. F. Bertsch and S. Das Gupta, Phys. Rept. **160**, 189 (1988); W. Cassing, V. Metag, U. Mosel, and K. Niita, *ibid.* **188**, 363 (1990); O. Buss *et al.*, *ibid.* **512**, 1 (2012).
[78] J. Aichelin and H. Stoecker, Phys. Lett. B **176**, 14 (1986); J. Aichelin, Phys. Rept. **202**, 233 (1991).
[79] P. Bozek and I. Wyskiel, Phys. Rev. C **81**, 054902 (2010).
[80] A. Adil, M. Gyulassy, and T. Hirano, Phys. Rev. D **73**, 074006 (2006).
[81] E. L. Bratkovskaya, W. Cassing, and H. Stöcker, Phys. Rev. C **67**, 054905 (2003).
[82] T. Hirano, U. W. Heinz, D. Kharzeev, R. Lacey, and Y. Nara, Phys. Lett. B **636**, 299 (2006).
[83] C. Nonaka and S. A. Bass, Phys. Rev. C **75**, 014902 (2007).
[84] C. Pinkenburg *et al.* (E895 Collaboration), Phys. Rev. Lett. **83**, 1295 (1999).